Chapter 4
Texture-Based Statistical Detection and Discrimination of Some Respiratory Diseases Using Chest Radiograph

Norliza Mohd Noor, Omar Mohd Rijal, Ashari Yunus, Aziah Ahmad Mahayiddin, Chew Peng Gan, Ee Ling Ong and Syed Abdul Rahman Abu Bakar

Abstract This chapter proposes a novel texture-based statistical procedure to detect and discriminate lobar pneumonia, pulmonary tuberculosis (PTB), and lung cancer simultaneously using digitized chest radiographs. A modified principal component method applied to wavelet texture measures yielded feature vectors for the statistical discrimination procedure. The procedure initially discriminated between a particular disease and the normals. The maximum column sum energy texture measure yielded 98 % correct classification rates for all three diseases. The diseases were then compared pair-wise, and the combination of mean of energy and maximum value texture measures gave correct classification rates of 70, 97, and 79 % for pneumonia, PTB, and lung cancer, respectively.

Keywords Digital chest radiographs · Statistical discrimination · Pneumonia · Pulmonary tuberculosis · Lung cancer

N. Mohd Noor (✉)
Razak School of Engineering and Advanced Technology, Universiti Teknologi Malaysia, UTM Kuala Lumpur Campus, Jalan Semarak, 54100 Kuala Lumpur, Malaysia
e-mail: norliza@utm.my

O. Mohd Rijal · C. P. Gan · E. L. Ong
Institute of Mathematical Science, University of Malaya, Lembah Pantai, 50603 Kuala Lumpur, Malaysia
e-mail: omarrija@um.edu.my

A. Yunus · A. A. Mahayiddin
Institute of Respiratory Medicine, Kuala Lumpur, Jalan Pahang 50586 Kuala Lumpur, Malaysia
e-mail: ashdr64@yahoo.com.au

S. A. R. Abu Bakar
Faculty of Electrical Engineering, Universiti Teknologi Malaysia, 81310 Skudai-Johor, Malaysia
e-mail: syed@fke.utm.my

K. W. Lai et al., *Advances in Medical Diagnostic Technology*, Lecture Notes in Bioengineering, DOI: 10.1007/978-981-4585-72-9_4,

4.1 Introduction

Tuberculosis and cancer are among the top killer diseases in the world where two million deaths worldwide are due to tuberculosis every year and about one million new cases of lung cancer have been detected annually (WHO 2003, 2006). In Malaysia, respiratory diseases accounted for 8.05 % of hospital admission with pneumonia being one of the top ten causes of death in Malaysian government hospital (Health Facts 2009). In 2008, the incidence rate of tuberculosis is 63.10 per 10,000 population and lung cancer incidence rate is 14.15 per 100,000 population for male and 6.1 per 100,000 for female (Health Facts 2009; Malaysian Cancer Statistics 2006). Lung cancer is third most common cancer among the population in Peninsular Malaysia (Malaysian Cancer Statistics 2006). The government's failure to curb smoking effectively contributes to high incidence of lung cancer especially in male population. The emergence of tuberculosis is partly due to the failure in diagnosing PTB patients seeking treatment for continuous cough (TB a Problem Once Again 2008). The similarity in terms of symptom and signs of the these three lung diseases makes diagnosing difficult for the medical practitioner.

Despite rapid advances in medical imaging technology, the conventional chest radiograph is still an important ingredient in the diagnosis of lung ailments (Ginnekien et al. 2001; Middlemiss 1982; Moores 1987). In Malaysia, government hospitals perform the diagnosis using radiograph films simply out of economic considerations.

The immediate problem with the use of chest X-rays concerns the use of considerable visual interpretation. Studies have shown that the accuracy of the interpretation is subject to varying degrees of observer error (Frieden 2004; Nakamura et al. 1970). This error includes the observer's inability to detect abnormal opacities and interpret them correctly, inter-observer variation (due to varying reading ability between observers) and intra-observer variation. The study done by Nakamura et al. (1970) stated that the observer error rates using radiograph images were high. Schillham et al. (2006) further confirmed that observer error still existed, and its rates were still high. Therefore, one of the important contribution of this study is the ability to reduce the error rates for detection. The need for computer-aided diagnosis (CAD), as a second opinion, for the medical practitioner is important in reducing the observer error.

In addition to the difficulty of using the conventional chest radiographs, there is an additional problem of the simultaneous discrimination for the three diseases. Related studies tend to address the problem of detecting and comparing a particular disease with normals. For example, Oliveira et al. (2007) studied the problem of pneumonia present and pneumonia absent using chest radiograph in detecting childhood pneumonia and van Ginneken et al. (2002) studied the problem of detecting pulmonary tuberculosis from mass TB screening program.

In using symptom and signs as the diagnosing tools, Hamilton et al. (2005) investigate clinical features used in detection of lung cancer and Gopi et al. (2007)

study the clinical features used in the diagnosis and treatment of tuberculous pleural effusion.

Simultaneous discrimination in the diagnosis of the three diseases is important when the prevalence of the three diseases is high. Effective and quick simultaneous screening will provide proper attention to the patient, and thus, the appropriate advanced test can be provided. This will eliminate the time-consuming diagnosis (eliminating disease one by one), currently practiced in most clinics. As far as this chapter is written, authors are not aware whether any studies have been done to discriminate the three diseases simultaneously.

A lot of work has been done on chest CAD algorithm for detection of lung nodules, interstitial opacities, cardiomegaly, vertebral fractures, interval changes in chest radiograph, classification of benign and malignant nodules, and the differential diagnosis of interstitial lung diseases (Schillham et al. 2006; Oliveira et al. 2007; van Ginneken et al. 2002; Hara et al. 2007).

Our proposed CAD algorithm is different from other semi-automatic methods in the sense that the selection of region of interest (ROI) does not involve the usual segmentation problem. The proposed statistical-based CAD algorithm does not depend on establishing precise boundaries. It is also not required to minimize any cost function associated with a given segmentation algorithm (Oliveira et al. 2007; van Ginneken et al. 2002; Hara et al. 2007; Katsuragawa and Doi 2007).

Similar studies in detecting lung abnormalities involving chest radiograph uses texture (Ginneken et al. 2002), contrast enhancement (Arzhaeva et al. 2009) and morphology features (Homma et al. 2009). Texture features in the form of moments of responses (standard deviation, skew, and kurtosis) extracted from multiscale filter banks for each ROI were considered in Ginneken et al. (2002). Their result showed a sensitivity of 0.86 at a specificity of 0.50 (area under the receiver operating curve is 0.820) in a TB mass screening program, which consist of 147 images with textural abnormalities and 241 were normal images, and a sensitivity of 0.97 at a specificity of 0.90 (area under the receiver operating curve is 0.986) when applied to a second database that consist of 100 normal images and 100 abnormal images. Arzhaeva et al. (2009) applied multiscale filter bank of Gaussian derivatives and obtained moments of histograms as texture features. The authors used dissimilarity-based classification, which resulted in an area of 0.98 under the receiver operating curve. Katsuragawa and Doi (2007) enhanced the image of lung nodules by a difference-image technique and hence applied a rule-based method as the classifier. Their result showed a recognition rate of 98.5 % for 1,681 cases, and even for 22 misfiled cases, 86.4 % were correctly identified. Homma et al. (2009) used morphological filters and achieved high true positive rate for their CAD system for detecting lung cancer using X-ray CT.

This study concentrates on developing the algorithm for feature extraction useful for differentiating lung diseases, which are very similar in clinical symptoms and sign, namely lobar pneumonia, pulmonary tuberculosis, and lung cancer. These features are the input to a novel discrimination procedure. The algorithm developed has been used to develop a semi-automated CAD system. It should be emphasized that the CAD was designed as a low cost system where the only

imaging modality utilized is the chest X-ray image, hence, other imaging modality such as MRI and volumetric CT were not considered.

Error rates are defined for the pair-wise discrimination of two types of diseases. For example, when discriminating between two types of lung conditions A_j and A_k, the error rates are given as:

$$\alpha = \mathrm{P}(\text{Type I Error}) = \mathrm{P}\left(A_j | A_k\right)$$
$$\beta = \mathrm{P}(\text{Type II Error}) = \mathrm{P}\left(A_k | A_j\right)$$

where $j \neq k$, $j = 1, \ldots, 4$, $k = 1, \ldots, 4$.

The infected region or ROI cannot be easily represented by standard measurement of length, area, shape, and size causing the selection of feature vectors difficult for any discrimination procedure. Henceforth, any standard image processing technique such as image enhancement or segmentation is avoided as much as possible to avoid possible lost of information from the original image.

4.2 Materials and Methods

4.2.1 Selection of Case Study

This study involved collaboration with the Institute of Respiratory Medicine (IPR), Malaysia, which is the national referral center for respiratory diseases. Cases that arrived at the IPR may be considered a random sample since an individual case may come from any of the Malaysian hospitals or clinics. The IPR provided archived patients' data which include chest X-ray films captured using the Phillips Diagnost 55/Super 50CP (Phillips Corp., Holland) together with complete patients' medical information. The patients' chest were captured in full inspiration using the posterior–anterior (PA) view with distance from the X-ray to the patient is fixed at 180 cm to diminish the effect of beam divergence and magnification of structures closer to the X-ray tube. The cassette size of 35×35 cm is used for female chest and 35×34 cm for male chest. The patient is exposed to 64 kV and 4.0 mAs if underweight, and 70 kV and 5.0 mAs if the patient has normal weight.

The archived data (stored in files) in IPR were diagnosed by a pulmonologist. In IPR, all the pulmonologists are trained to interpret chest radiographs. Stratified random sampling (SRS) was carried out for the patients' file. SRS means that files were randomly selected given that the patients chosen were already diagnosed as PTB or LC. The role of the consultant pulmonologist is to verify the diagnosis. It should be noted that the pulmonologist and consultant pulmonologist mentioned above are two different individuals.

The patient's chest X-ray is then divided into two groups, which are the control group and the test group. The selected patients used as the control group were the confirmed pneumonia (PNEU), pulmonary tuberculosis (PTB), and lung cancer (LC)

cases with no other systemic diseases such as diabetes, hypertension, and heart disease. The omission of cases with other systemic diseases was done in order to avoid bias in the development of the statistical discriminant function (DF). The test group was selected similarly except that some of the patients may have other systemic diseases.

Lobar pneumonia is defined when one section or lobe of the lung is affected. In diagnosing pneumonia, the patient is assessed for crackles and wheezing sound from the lung, using a stethoscope (Wipf et al. 1999). The radiographic interpretation is considered the gold standard for the presence of pneumonia where the physical findings is accurate if it is found in the same location as an infiltrate on chest X-ray (Wipf et al. 1999). The confirmation of the PTB cases is based on the clinical feature (symptoms and sign), chest X-ray examination, and sputum Acid Fast Bacilli (AFB) direct smear. For the lung cancer, cases under study consist of 75 % cases of non-small cell carcinoma (of which 50 % are the squamous cell carcinoma and 25 % are the adenocarcinoma) and 25 % cases of small cell carcinoma. The confirmation of LC was based on bronchial biopsy result. The normal lung (NL) chest X-ray films selected by the radiologist from Universiti Sains Malaysia Hospital (HUSM) represent patients who came for a general medical checkup.

Patients that have lung disease (either PNEU, PTB, or LC) will have their chest X-ray film image shows some abnormal opacity. The existence of lung consolidation in the chest X-ray may confirm the existence of pneumonia and may appear on the chest X-ray after a few days of infection. The PTB image will show multiple opacities of varying size that run together (coalesce) in the chest X-ray image. Severe cases of PTB may result in consolidation and cavity, and the scarring marks may remain visible in the chest X-ray even after the patient is cured. Lung cancer appears as a mass opacity in the chest X-ray image. The chest radiograph image of a normal lung will show a complete dark image between rib bones due to nonexistence of any hardened substances.

The chest X-ray films were then digitized into DICOM format using the Kodak LS 75 X-ray Film Scanner (pixel spot size of 100 μm, 12 bit per pixel, image size of 2016 × 2048 pixels). An example of a digitized X-ray film is shown in Fig. 4.1a–d.

4.2.2 Texture Measures

Each of the ROI for a given image was subjected to the two-dimensional Daubechies wavelet transform as shown in Fig. 4.2, (Daubechies 1992; Walker 1999). The wavelet transform convert the image into four subsets, labeled LL, LH, HL, and HH representing the trend, horizontal, vertical, and diagonal detail coefficients.

The twelve texture measures considered were as follows:

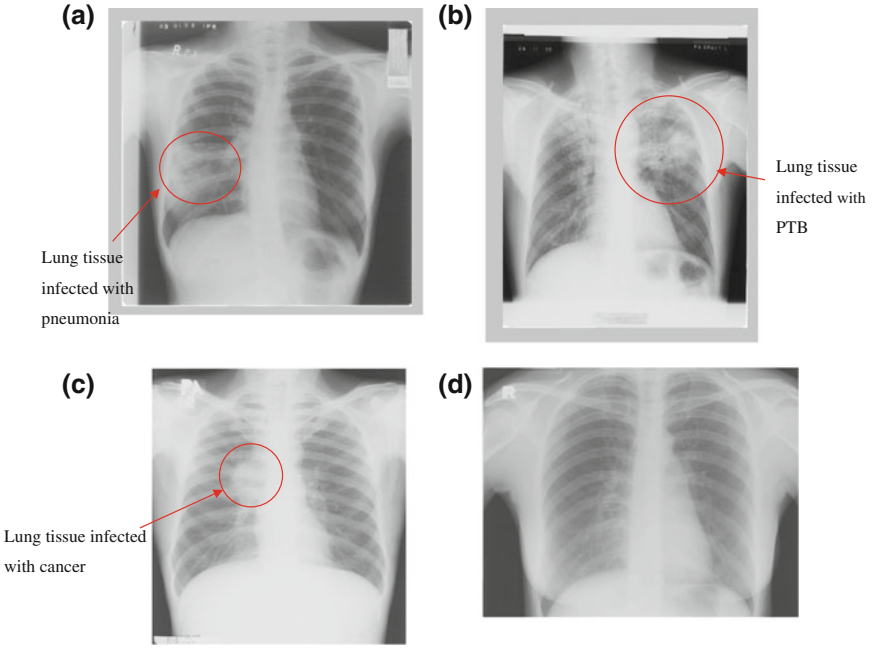

Fig. 4.1 **a** Visual of chest radiograph of pneumonia-infected lung (*source* The Institute of Respiratory Medicine, Kuala Lumpur). **b** Example of chest radiograph showing PTB-infected lung (snowflakes) (*source* The Institute of Respiratory Medicine, Kuala Lumpur). **c** Example of chest radiograph showing lung cancer (*source* The Institute of Respiratory Medicine, Kuala Lumpur). **d** Example of normal lung of an healthy individual (*source* The Institute of Respiratory Medicine, Kuala Lumpur)

1. Mean Energy, $E = \frac{1}{N}\sum_j \sum_k |C_{jk}|^2$
2. Entropy $= -\frac{1}{N^2}\sum_j \sum_k |C_{jk}|^2 \log |C_{jk}|^2$
3. Contrast $= \sum_j \sum_k (j-k)^2 C_{jk}$
4. Homogeneity, $H = \sum_j \sum_k \frac{C_{jk}}{1+|j-k|}$
5. Standard deviation of value, $\text{STDV} = \sqrt{\frac{1}{N^2}\sum_j \sum_k (C_{jk}-\mu)^2}$ where $\mu = \frac{1}{N^2}\sum_j \sum_k C_{jk}$
6. Standard deviation of energy, $\text{STDE} = \sqrt{\frac{1}{N^2}\sum_j \sum_k \left(|C_{jk}|^2 - \mu\right)^2}$ where $\mu = \frac{1}{N^2}\sum_j \sum_k |C_{jk}|^2$
7. Maximum wavelet coefficient value, $\max = \max(C_{jk})$
8. Minimum wavelet coefficient value, $\min = \min(C_{jk})$
9. Maximum value of energy, $E_{\max} = \max\left(\sum_j \sum_k |C_{jk}|^2\right)$
10. Maximum row sum energy

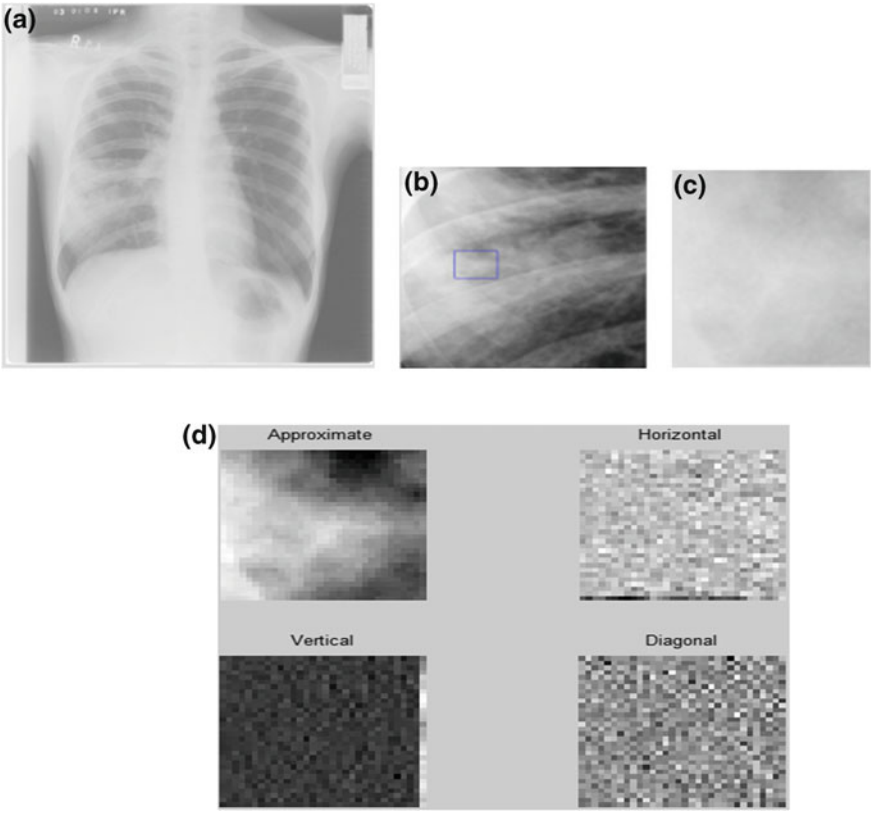

Fig. 4.2 **a** Chest X-ray of a pneumonia patient and **b** a subset image of the infected area. **c** Region of interest and **d** the transformed image where four image subset was formed (*source* The Institute of Respiratory Medicine, Kuala Lumpur)

11. Maximum column sum energy
12. Average number of zero-crossings

where C_{jk} is the element of sub-image (say, LL) found in row-j and column-k (Gonzalez and Woods 1992; Sonka et al. 1998). Hence, twelve texture measures in each of LL, LH, HL, and HH yield 48 descriptors or features, $\underline{u}$, that will be used to detect pneumonia.

4.2.3 Modified Principal Component Method

The modified principal component (ModPC) method was introduced in (Noor et al. 2010) where PNEU is discriminated from normals. The ModPC method is now extended for pair-wise comparison between three types of diseases namely, PNEU, PTB, LC, and normals.

A sample of 200 images were concurrently read and interpreted for the presence of PNEU, PTB, LC, and normals by two independent pulmonologists who are trained according to the World Health Organization (WHO) guideline (WHO Report 2004; Cherian et al. 2005), and the affected region (ROI) was identified.

The data used were divided into two sets, $(\underline{u}_1, \underline{u}_2, \ldots, \underline{u}_{120})$ as the control data set and $(\underline{u}_{121}, \underline{u}_{122}, \ldots, \underline{u}_{200})$ as the test data set. Let,

$\underline{u}_1, \underline{u}_2, \ldots, \underline{u}_{30}$ where $\underline{u} \in G_1$ represents the texture measures for PNEU samples,
$\underline{u}_{31}, \underline{u}_{32}, \ldots, \underline{u}_{60}$ where $\underline{u} \in G_2$ represents the texture measures for normal lung samples,
$\underline{u}_{61}, \underline{u}_{62}, \ldots, \underline{u}_{90}$ where $\underline{u} \in G_3$ represents the texture measures for PTB samples, and $\underline{u}_{91}, \underline{u}_{92}, \ldots, \underline{u}_{120}$ where $\underline{u} \in G_4$ represents the texture measures for LC samples.

The main problem of the ModPC method is the choice of an orthogonal transformation. Let M be an orthogonal matrix such that

$$\underline{u}_r^* = M\underline{u}_r \ (r = 1, \ldots, 200).$$

Let $\frac{1}{n-1}S_j$ be the estimate of the covariance matrix for group G_j ($j = 1, \ldots, 4$). For example,

$$S_1 = \sum_{r=1}^{30} (\underline{u}_r - \overline{\underline{u}})(\underline{u}_r - \overline{\underline{u}})^T \quad \text{where } \overline{\underline{u}} = (\underline{u}_1 + \underline{u}_2 + \cdots + \underline{u}_{30})/30$$

while S_2, S_3, and S_4 were similarly defined for the sets G_2, G_3, and G_4, respectively.

The spectral decomposition of the estimated covariance matrices are

$$\frac{1}{n-1}S_j = Q_j \Lambda_j Q_j^T \quad \text{for } G_j \ (j = 1, 2, 3, 4)$$

where $n = 30$, $Q_j (j = 1, \ldots, 4)$ is the appropriate matrix of eigenvectors, and Λ_j ($j = 1, \ldots, 4$) is the corresponding diagonal matrix of eigenvalues. Henceforth, the choice of M will depend on minimizing misclassification probabilities in a two population discrimination problems. In particular, choose $M = Q_j$ or $M = Q_k$ ($j \neq k$), $j = 1, \ldots, 4$ and $k = 1, \ldots, 4$ such that the probability of misclassifying the test data to either population-j or population-k is minimized.

Without loss of generality, consider the two population discrimination problems PNEU and NL. For a selected M matrix, take the first two components of $\underline{u}_r^* (r = 1, \ldots, 30)$, which explain at least 90 % of the variability, relabel it as $\underline{v}_r$ ($r = 1, \ldots, 30$), and perform the following:

For vectors, $\underline{v}_1, \underline{v}_2, \ldots, \underline{v}_{30}, \in \Re^2$ calculate the statistics $\overline{\underline{v}}_1 = (\underline{v}_1 + \cdots + \underline{v}_{30})/30$ and $S_{v1} = \sum_{j=1}^{30} \left(\underline{v}_j - \overline{\underline{v}}_1\right)\left(\underline{v}_j - \overline{\underline{v}}_1\right)^T$. The vectors $\underline{v}_1, \underline{v}_2, \ldots, \underline{v}_{30}$ were found to be bivariate normal (see Sect. 4.2.4). Henceforth, the PNEU ellipsoid $(\underline{v} - \overline{\underline{v}}_1)^T\left((n-1)S_{v1}^{-1}\right)(\underline{v} - \overline{\underline{v}}_1) = c$ was drawn where c was selected from a standard

Chi square table (see Sect. 4.2.5). Further, the estimate of $g_1(\underline{v})$, which is the probability distribution for G_1 was also obtained.

The above was repeated for $\underline{v}_{31}$, $\underline{v}_{32}$, …, $\underline{v}_{60}$ yielding, say the NL ellipsoid and the corresponding estimate of $g_2(\underline{v})$ which is the probability distribution for G_2. Finally, the estimate of the discriminant function $\mathrm{DF}_{12}(\underline{v}) = \ln\frac{g_1(\underline{v})}{g_2(\underline{v})}$ may be derived (Johnson and Wichern 2007). Two-dimensional probability ellipsoids and appropriate DFs estimate the following error probability;

$$\alpha = \mathrm{P}(\text{Type 1 Error}) = \mathrm{P}(\text{PNEU}|\text{NL}) \tag{4.1}$$

and

$$\beta = \mathrm{P}(\text{Type 2 Error}) = \mathrm{P}(\text{NL}|\text{PNEU}) \tag{4.2}$$

for a selected texture measure.

For the PNEU–NL discrimination problem, there are two ways of estimating the error probabilities α and β by using the test set $\underline{v}_{121}$, $\underline{v}_{62}$, …, $\underline{v}_{140}$ from G_1 and $\underline{v}_{141}$, $\underline{v}_{82}$, …, $\underline{v}_{160}$ from G_2 in two ways where $\underline{v}_j$ $(j = 121, \ldots, 160)$ are the first two components of $\underline{u}_r^* = M\underline{u}_r = Q\underline{u}_r (r = 121, \ldots, 160)$;

(a) Estimation of α and β from the probability ellipsoid:

1. The number of times $\underline{v}_j$ $(j = 121, \ldots, 140)$ falls into the NL ellipsoid gives an estimate of β.
2. The number of times $\underline{v}_j$ $(j = 141, \ldots, 160)$ falls into the PNEU ellipsoid gives an estimate of α.

(b) Estimation of α and β from DF:

Investigate if $\mathrm{DF}_{12}(\underline{v}) = \ln\frac{g_1(\underline{v})}{g_2(\underline{v})} < \log K$

where $g_1(\underline{v})$, the probability distribution for PNEU, was found to be $N_2(\underline{\mu}_1, \Sigma_1)$ and $g_2(\underline{v})$, the probability distribution for NL was shown to be $N_2(\underline{\mu}_2, \Sigma_2)$. Further, $K = \frac{d(1|2)}{d(2|1)}\frac{p_2}{p_1}$ where $d(i|j)$ is the cost of misclassifying observation-j ($i = 1, 2$ and $j = 1, 2$), while p_1 and p_2 are the a priori probabilities. Suppose $\underline{v}^*$ is an unknown observation and assuming that $p_1 = p_2$ and $d(1|2) = d(2|1)$, then $\underline{v}^*$ is assigned to the PNEU group if $\mathrm{DF}_{12}(\underline{v}^*) > 0$, otherwise it is assigned to the NL group.

The equality of covariance matrices was tested using the Box's Test (Mardia et al. 1979), and if $\Sigma_1 = \Sigma_2$, $\mathrm{DF}_{12}(\underline{v})$ is the linear discriminant function (LDF), which allocates the unknown observation $\underline{m}_0$ as follows;

Allocate $\underline{m}_0$ to population one if

$$\left[(\underline{\mu}_1 - \underline{\mu}_2)^T \Sigma^{-1}(\underline{m}_0) + \frac{1}{2}(\underline{\mu}_1 - \underline{\mu}_2)^T \Sigma^{-1}(\underline{\mu}_1 + \underline{\mu}_2)\right] \geq \ln\left[\left(\frac{d(1|2)}{d(2|1)}\right)\left(\frac{p_2}{p_1}\right)\right] \tag{4.3}$$

Table 4.1 Pair-wise discrimination strategy between disease absent (DA) and disease present (DP)

Pair-wise component	Type I error	Type II error
Pneumonia–normal lung (PNEU–NL)	P(PNEU|NL)	P(NL|PNEU)
Pulmonary tuberculosis–normal lung (PTB–NL)	P(PTB|NL)	P(NL|PTB)
Lung Cancer–normal lung (LC–NL)	P(LC|NL)	P(NL|LC)

Table 4.2 Pair-wise discrimination strategy between diseases

Pair-wise component	Type I error	Type II error
PNEU–PTB	P(PNEU|PTB)	P(PTB|PNEU)
PNEU–LC	P(PNEU|LC)	P(LC|PNEU)
PTB–LC	P(PTB|LC)	P(LC|PTB)

Otherwise allocate $\underline{m}_0$ to population two.

Alternatively, if $\Sigma_1 \neq \Sigma_2$ then $\mathrm{DF}_{12}(\underline{v})$ is the quadratic discriminant function (QDF), which allocates the unknown $\underline{m}_0$ as follows;

Allocate $\underline{m}_0$ to population one if

$$\left[-\frac{1}{2}\underline{m}_0^T\Sigma_1^{-1} - \Sigma_2^{-1}\underline{m}_0 + (\underline{\mu}_1^T\Sigma_1^{-1} - \underline{\mu}_2^T\Sigma_2^{-1})^T\underline{m}_0 - k\right] \geq \left(\frac{d(1|2)}{d(2|1)}\right)\left(\frac{p_2}{p_1}\right) \quad (4.4)$$

where $k = \frac{1}{2}\ln\left(\frac{|\Sigma_1|}{|\Sigma_2|}\right) + \frac{1}{2}\left(\underline{\mu}_1^{T|}\Sigma_1^{-1}\underline{\mu}_1 - \underline{\mu}_2^{T|}\Sigma_2^{-1}\underline{\mu}_2\right)$.

Otherwise allocate $\underline{m}_0$ to population two.

Throughout the study it is assumed that $d(1|2) = d(2|1)$ and $p_1 = p_2$ for both Eqs. 4.3 and 4.4. These assumptions were taken because the event of having either disease is regarded with having equal weight, and equal a prior probability is because there is no true or exact information about total frequency of cases in Malaysia.

Henceforth, the number of times $\mathrm{DF}_{12}(\underline{v}_j) < 0$ for $\underline{v}_j$ $(j = 121, \ldots, 140)$ gives an estimate of β. Likewise, α is similarly derived.

All the above were repeated for the second selection of M (say $M = Q_k$) and suppose this choice yields lower α and β values, then $M = Q_k$ will be the preferred choice. Tables 4.1 and 4.2 illustrate all the combination of the two population discrimination problem studied. Flowchart shown in Fig. 4.3 illustrates the discrimination problem for the disease present and disease absent cases. Flowchart shown in Fig. 4.4 gives similar illustration for the pair-wise comparison of diseases.

4.2.4 Testing for Normality

Given $\underline{v}_1, \underline{v}_2, \ldots, \underline{v}_n \in \Re^2$. The statistics $\overline{\underline{v}} = (\underline{v}_1 + \cdots + \underline{v}_n)/n$ and $S_v = \sum_{j=1}^{n}(\underline{v}_j - \overline{\underline{v}})(\underline{v}_j - \overline{\underline{v}})^T$ and $y_j = (\underline{v}_j - \overline{\underline{v}})^T\left((n-1)S_v^{-1}\right)(\underline{v}_j - \overline{\underline{v}})$ for $j = 1, \ldots, n$ were

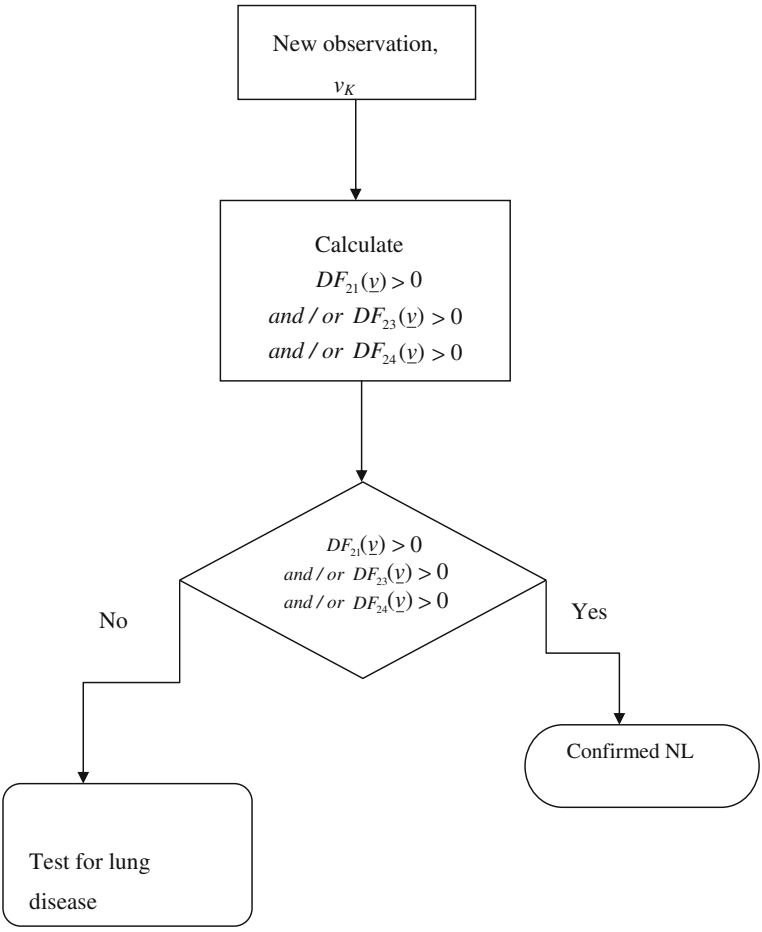

Fig. 4.3 The discrimination procedure flowchart for discriminating disease present and disease absent

calculated. If $\underline{v}_j$ is normally distributed, then y_j ($j = 1, \ldots, n$) must come from a Chi squared distribution with two degrees of freedom. Effectively, testing normality of $\underline{v}_1, \underline{v}_2, \ldots, \underline{v}_n$ is equivalent to testing whether y_j $(j = 1, \ldots, n)$ comes from a Chi squared distribution using the Kolgomorov–Smirnov test, (Mardia et al. 1979). In all cases studied, the Kolmogorov–Smirnov test confirms that y_j has a Chi squared distribution, henceforth, indicating that $\underline{v}_j$ is bivariate normal.

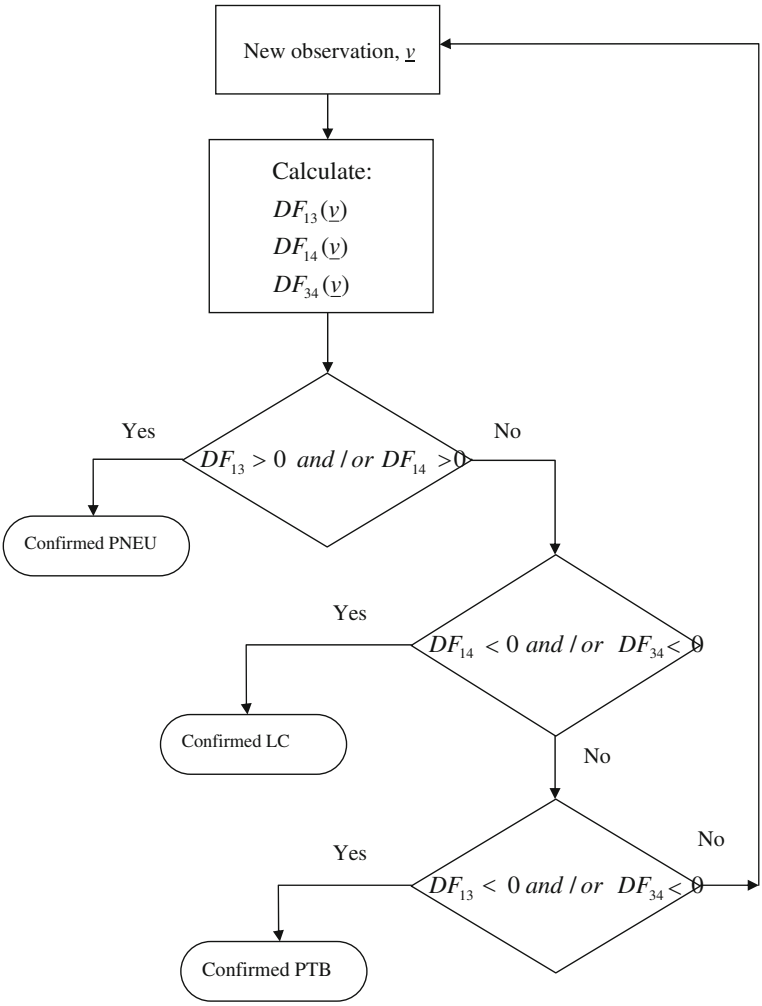

Fig. 4.4 The discrimination procedure flowchart for discriminating PNEU, PTB, and LC

4.2.5 Confidence Region of the First Two Components of $\underline{v}$

A 2D plot of the first two components of $\underline{v}$ together with its corresponding approximate confidence region (an ellipse) was used to investigate clustering of the two groups of individuals. If two clusters of points are discovered on the 2D plot and each cluster is contained in a separate confidence ellipse then the texture measures used ($\underline{u}$) is regarded as a useful feature for discrimination. The 95 % probability ellipsoid was drawn for each group.

Since $\underline{v}$ is bivariate normal, therefore a value for c may be selected from standard Chi squared tables. The quadratic form, for example, $(\underline{v} - \overline{\underline{v}}_1)^T \left((n-1)S_1^{-1}\right)(\underline{v} - \overline{\underline{v}}_1)$ is approximately a Chi squared random variable where the approximation is considered good if $n \geq 25$, (Andrews 1972).

4.2.6 Discrimination Strategy

The main strategy of the current statistical discrimination procedure is to detect normal healthy individuals (NL) first, those not categorized as NL would then be tested as being either PNEU, PTB, or LC.

4.2.6.1 Discrimination Between Disease Present and Disease Absent (NL)

Using two-dimensional wavelet transformation, a selected ROI will generate four components, namely the approximate (LL), vertical (LH), horizontal (HL), and diagonal (HH) components. In each of these four components, twelve texture measures are calculated, yielding 48 descriptors or features. Preliminary explanatory data analysis (EDA) using two-dimensional plots for a given pair of features does not provide obvious separation between clusters. This suggests that the choice of features is non-trivial. Henceforth, a modified principal component (modPC) method is proposed.

In the modPC method, a feature vector, say $\underline{v}$, is selected in two ways. Firstly, each patient's ROI is represented by a four-dimensional vector, for example, entropy LL, entropy LH, entropy HL, and entropy HH. This approach is to investigate the capability of each texture measure as the texture descriptor for each type of disease. The second approach is to use all 12 texture measures (48 dimensional feature vectors). By combining all twelve texture measures, a superior texture descriptor is hoped to be able to represent each disease. In either approach, the appropriate Q matrix is first derived before the principal component (PC) is applied onto it. This method named as the modified PC (modPC) method was successfully applied in the discrimination between PNEU and NL (Noor et al. 2010).

The discrimination strategy between DP and DA, for the three cases PNEU–NL, PTB–NL, and LC–NL required that the feature vector $\underline{v}$ is subjected to the following constrains. In particular, if the DF is such that,

$$\mathrm{DF}_{21}(\underline{v}) = \ln \frac{g_2(\underline{v})}{g_1(\underline{v})} > 0 \tag{4.5}$$

and,

$$\mathrm{DF}_{23}(\underline{v}) = \ln \frac{g_2(\underline{v})}{g_3(\underline{v})} > 0 \tag{4.6}$$

and,

$$\mathrm{DF}_{24}(\underline{v}) = \ln \frac{g_2(\underline{v})}{g_4(\underline{v})} > 0 \tag{4.7}$$

where the integers 1, 2, 3, and 4 represent PNEU, NL, PTB, and LC, respectively, then $\underline{v}$ is said to represent a patient that has a normal lung.

Note that DF($\underline{v}$) is either the LDF($\underline{v}$) or QDF($\underline{v}$), a choice made after testing for $\Sigma_1 = \Sigma_2$. To reduce the cost of misclassification, three ROIs for each patient were considered. Another purpose of taking three areas for each patient is to ensure that the texture descriptor is homogeneous in the ROI.

4.2.6.2 Discriminating Between Diseases: PNEU, PTB, and LC

Despite the optimistic results of the previous section, any attempt to discriminate PNEU–PTB, PNEU–LC, or PTB–LC will not necessarily yield similar results. This is due to the fact that the abnormal appearance for these diseases on the X-ray film is very similar (Adam and Dixon 2008).

The results showing the lowest misclassification rates are summarized in Table 4.6. Following De Veaux et al. (2009), for a particular pair-wise comparison, the error measure with lowest value will be used as an indicator of performance. In Table 4.6, type II error was used for the PNEU–PTB and PTB–LC comparison, while for the PNEU–LC, type I error was used. The texture measure that gives the lowest error rates for both types of Q matrix will be selected. In particular, when both error rates are similar or equal the choice of Q matrix is arbitrary.

The proposed discrimination procedure is as follows;

Given $\underline{v}$ calculate;

$$\mathrm{DF}_{13}(\underline{v}) = \ln \frac{f_{\mathrm{PNEU}}(\underline{v})}{f_{\mathrm{PTB}}(\underline{v})}, \text{ utilizing } Q_{\mathrm{PTB}} \tag{4.8}$$

$$\mathrm{DF}_{14}(\underline{v}) = \ln \frac{f_{\mathrm{PNEU}}(\underline{v})}{f_{\mathrm{LC}}(\underline{v})}, \text{ utilizing } Q_{\mathrm{LC}} \tag{4.9}$$

$$\mathrm{DF}_{34}(\underline{v}) = \ln \frac{f_{\mathrm{PTB}}(\underline{v})}{f_{\mathrm{LC}}(\underline{v})}, \text{ utilizing } Q_{\mathrm{PTB}} \tag{4.10}$$

Suppose $\underline{v}_o$ is an unknown observation (see Fig. 4.4),

$$\text{If } \mathrm{DF}_{13}(\underline{v}_o) > 0 \quad \text{and/or} \quad \mathrm{DF}_{14}(\underline{v}_o) > 0 \Rightarrow v_o \in \text{PNEU} \tag{4.11}$$

$$\text{If } \mathrm{DF}_{14}(\underline{v}_o) < 0 \quad \text{and/or} \quad \mathrm{DF}_{34}(\underline{v}_o) < 0 \Rightarrow \underline{v}_o \in \text{LC} \tag{4.12}$$

$$\text{If } \mathrm{DF}_{13}(\underline{v}_o) < 0 \quad \text{and/or} \quad \mathrm{DF}_{34}(\underline{v}_o) > 0 \Rightarrow \underline{v}_o \in \text{PTB} \tag{4.13}$$

The above discrimination procedure can be used in two ways. Firstly, the individual Eqs. 4.8–4.10 yields the discrimination problem when only two types of diseases are of interest, for example, Eq. 4.10 should be applied when the interest is only in comparing PTB and LC. The set of conditions determined by Eqs. 4.11–4.13 gives the three population discrimination problem which constitutes the second discrimination procedure.

To increase the test sample size, each ROI is now treated as coming from a separate individual, giving a maximum of 60 counts of possible successful detection (sample size is 20). The selection of ROI was done in similar fashion as in Sect. 4.2.6.1.

4.3 Result

The pair-wise discrimination strategy between disease present (DP) and disease absent (DA) shows that the type I error and type II error were less than 15 % when maximum column sum energy texture descriptor are applied for PNEU–NL, PTB–NL, and LC–NL regardless which Q is used (see Table 4.3). It is interesting to note that when maximum column sum energy is jointly used with the other 11 texture measures the error probability may increase (see last row of Table 4.3). The discrimination procedure using either (or all) of $\mathrm{DF}_{21}(\underline{v})$, $\mathrm{DF}_{23}(\underline{v})$, or $\mathrm{DF}_{24}(\underline{v})$, shown in Fig. 4.3, shows the highest rates of correct classification when utilizing maximum column sum energy and Q_{NL} and is illustrated in Tables 4.4 and 4.5.

For the PNEU–PTB discrimination problem (Table 4.6) using Q_{PTB} and mean of energy and maximum value texture measures give lowest type II error rates. Both texture measures also give lowest error rates for the PNEU–LC and PTB–LC comparisons.

For the three population discrimination problems (Fig. 4.4) only the following case will be discussed;

Select $\underline{v}_o$ from the test set (all three diseases),if

$$\mathrm{DF}_{13}(\underline{v}_o) > 0 \quad \text{and} \quad \mathrm{DF}_{14}(\underline{v}_o) > 0 \quad \text{implies } \underline{v}_o \in \text{PNEU}$$

else if,

$$\mathrm{DF}_{14}(\underline{v}_o) < 0 \quad \text{and} \quad \mathrm{DF}_{34}(\underline{v}_o) < 0 \quad \text{implies } \underline{v}_o \in \text{LC}$$

else,

$$\mathrm{DF}_{13}(\underline{v}_o) < 0 \quad \text{and} \quad \mathrm{DF}_{34}(\underline{v}_o) > 0 \quad \text{implies } \underline{v}_o \in \text{PTB}$$

Table 4.3 Results of pair-wise discrimination for LC–NL, PTB–NL, and PNEU–NL

	Test group (from LDF/QDF)				Test group (from LDF/QDF)				Test group (from LDF/QDF)			
	Qnl		Qlc		Qnl		Qptb		Qnl		Qpneu	
	P(LC|NL)	P(NL|LC)	P(LC|NL)	P(NL|LC)	P(PTB|NL)	P(NL|PTB)	P(PTB|NL)	P(NL|PTB)	P(PNEU|NL)	P(NL|PNEU)	P(Pneu|NL)	P(NL|PNEU)
Mean of energy	0.00	0.20	0.35	0.05	0.90	0.10	0.90	0.10	0.5000	0.2500	0.8000	0.1000
Entropy	0.00	0.15	0.00	0.25	0.60	0.00	0.55	0.30	0.3500	0.3000	0.3000	0.4000
Standard deviation of intensity value	0.00	0.05	0.00	0.15	0.70	0.75	0.70	0.70	0.0500	0.3000	0.0500	0.3500
Standard deviation of energy	0.00	0.20	0.20	0.10	1.00	0.10	1.00	0.10	1.0000	0.0500	0.9000	0.0500
Maximum value	0.00	0.15	0.00	0.10	0.05	0.10	0.00	0.10	0.1000	0.1500	0.1000	0.0000
Minimum value	0.35	0.10	0.30	0.10	0.85	0.05	0.70	0.10	0.7500	0.2000	0.6500	0.2500
Maximum energy	0.05	0.10	0.00	0.10	0.15	0.10	0.20	0.10	0.1500	0.1000	0.1000	0.1000

(continued)

Table 4.3 (continued)

	Test group (from LDF/QDF)				Test group (from LDF/QDF)				Test group (from LDF/QDF)			
	Qnl		Qlc		Qnl		Qptb		Qnl		Qpneu	
	P(LC|NL)	P(NL|LC)	P(LC|NL)	P(NL|LC)	P(PTB|NL)	P(NL|PTB)	P(PTB|NL)	P(NL|PTB)	P(PNEU|NL)	P(NL|PNEU)	P(Pneu|NL)	P(NL|PNEU)
Maximum row sum energy	0.70	0.00	0.70	0.00	0.05	0.15	0.05	0.15	0.1000	0.1500	0.1000	0.1500
Maximum column sum energy	0.05	0.05	0.05	0.05	0.15	0.05	0.15	0.05	0.1500	0.1000	0.1000	0.1000
Zero-crossing	0.00	0.65	0.15	0.90	0.10	0.85	0.30	0.85	0.4500	0.6000	0.0500	0.7500
Contrast	0.90	0.00	0.05	0.10	0.15	0.10	0.25	0.10	0.8500	0.1000	0.1500	0.1500
Homogeneity	0.90	0.00	0.90	0.00	0.95	0.00	0.95	0.00	0.9000	0.0000	0.9000	0.0000
12 Features	0.00	0.10	0.00	0.10	0.30	0.10	0.35	0.10	0.2000	0.1000	0.2500	0.0000

Table 4.4 Correct classification rates for discriminating disease absent (DA) using NL test cases

Texture measure	Maximum column sum energy and Q_{NL}			
Discrimination procedure using NL test data set	$DF_{21} > 0$	$DF_{23} > 0$	$DF_{24} > 0$	$DF_{21} > 0$ and $DF_{23} > 0$ and $DF_{24} > 0$
Percentage correct classification (%)	65	70	98.33	65

Table 4.5 Correct classification results for discriminating disease present (DP) using PNEU, PTB, and LC test cases

Texture measure	Maximum column sum energy and Q_{NL}			
Discrimination procedure	$DF_{21} < 0$	$DF_{23} < 0$	$DF_{24} < 0$	$DF_{21} > 0$ and $DF_{23} > 0$ and $DF_{24} > 0$
PNEU test data set (%)	100	–	–	95
PTB test data set (%)	–	98.3	–	95
LC test data set (%)	–	–	98.3	98.3

When all three conditions are not satisfied the next member of the test set was considered. The above procedure yields 30 % correct classification for PNEU, and 95 % correct classification for PTB and 50 % correct classification for LC.

If the condition in the above procedure is relaxed, for example, if either $DF_{13}(\underline{v}_o) > 0$ or $DF_{14}(\underline{v}_o) > 0$ is satisfied, PNEU was found to be detected with higher correct classification rates (see Tables 4.7, 4.8 and 4.9). In particular, the relaxed condition yields correct classification rates of 70 % for PNEU, 97 % for PTB, and 79 % for LC.

4.4 Discussion

In the medical literature disease detection using chest radiograph is generally confined to the case of comparing (detection) a particular disease with normals. This study investigate the same problem but for three diseases (simultaneously). The results from this study suggest that the proposed statistical discrimination procedure can be used to detect either of PNEU, PTB, and LC when the comparison is made with normals yielding results that are comparable with similar studies (Oliveira et al. 2007; Katsuragawa and Doi 2007; Arzhaeva et al. 2009; Homma et al. 2009).

In the situation where two diseases are suspected, mean of energy or maximum value texture measures can be used for discrimination. Further, the choice of Q matrix is arbitrary.

Table 4.6 Misclassification using LDF/QDF for pair-wise discrimination for PNEU–PTB, PNEU–LC, and PTB–LC

Pair-wise	PNEU–PTB		PNEU–LC		PTB–LC	
Type of Q	Q_{PNEU}	Q_{PTB}	Q_{PNEU}	Q_{LC}	Q_{PTB}	Q_{LC}
Type of error/texture measures	P(type II error) = P (PTB|PNEU)	P(type II error) = P (PTB|PNEU)	P(type I error) = P (PNEU|LC)	P(type I error) = P (PNEU | LC)	P(type II error) = P(PTB|LC)	P(type II error) = P(PTB|LC)
Mean of energy	0.2000	0.2000	0.25	0.25	0.20	0.25
Entropy	0.3000	0.3000	0.25	0.25	0.20	0.20
Standard deviation of intensity value	0.4000	0.2500	0.20	0.35	0.25	0.10
Standard deviation of energy	0.3500	0.4500	0.30	0.35	0.25	0.35
Maximum value	0.6000	0.1500	0.15	0.15	0.15	0.25
Minimum value	0.4500	0.4500	0.25	0.25	0.25	0.25
Maximum energy	0.3500	0.2500	0.25	0.25	0.25	0.25
Maximum row sum energy	0.2000	0.2000	0.25	0.25	0.20	0.20
Maximum column sum energy	0.3000	0.3000	0.30	0.30	0.35	0.35
Zero-crossing	0.4500	0.2000	0.45	0.95	0.20	0.25
Contrast	0.5500	0.4000	0.25	0.20	0.20	0.25
Homogeneity	0.6000	0.4000	0.20	0.25	0.15	0.10
12 Features	0.4500	0.5000	0.25	0.25	0.35	0.15

Table 4.7 Correct classification results for PNEU

Wavelet texture measure	Mean of energy		Maximum value	
Discrimination procedure	$DF_4(\underline{x})$	$DF_5(\underline{x})$	$DF_4(\underline{x})$	$DF_5(\underline{x})$
Correct classification	14/60 (23.3 %)	23/60 (38.3 %)	38/60 (63.3 %)	23/60 (38.3 %)
Combine (satisfy either $DF_4(\underline{x}) > 0$ or $DF_5(\underline{x}) > 0$)	26/60 (43.3 %)		40/60 (66.67 %)	
Combine all (satisfy either $DF_4(\underline{x}) > 0$ or $DF_5(\underline{x}) > 0$ for both texture measures)	42/60 (70 %)			

Table 4.8 Correct classification results for PTB

Wavelet texture measure	Mean of energy		Maximum value	
Discrimination procedure	$DF_4(\underline{x})$	$DF_6(\underline{x})$	$DF_4(\underline{x})$	$DF_6(\underline{x})$
Correct classification	51/60 (85 %)	55/60 (91.67 %)	13/60 (21.67 %)	17/60 (28.33 %)
Combine (satisfy either $DF_4(\underline{x}) < 0$ or $DF_6(\underline{x}) > 0$)	55/60 (91.67 %)		20/60 (33.33 %)	
Combine all (satisfy either $DF_4(\underline{x}) < 0$ or $DF_6(\underline{x}) > 0$ for both texture measures)	58/60 (96.67 %)			

Table 4.9 Correct classification results for LC

Wavelet texture measure	Mean of energy		Maximum value	
Discrimination procedure	$DF_5(\underline{x})$	$DF_6(\underline{x})$	$DF_5(\underline{x})$	$DF_6(\underline{x})$
Correct classification	27/42 (64.3 %)	3/42 (7.14 %)	24/42 (57.1 %)	27/42 (64.3 %)
Combine (satisfy either $DF_5(\underline{x}) < 0$ or $DF_6(\underline{x}) < 0$)	29/42 (69 %)		31/42 (73.8 %)	
Combine all (satisfy either $DF_5(\underline{x}) < 0$ or $DF_6(\underline{x}) < 0$ for both texture measures)	33/42 (78.6 %)			

In the three population discrimination problems, it is not expected for the strict discrimination procedure to yield a high success rate for all three diseases. This must be due to the fact that the diseases may appear to be similar on the chest radiographs. In particular, the procedure must be modified, for example, use other texture measure to allow better detection rates for PNEU and LC. However, if

more relaxed constraints on the discrimination procedure were allowed, higher correct classification rates can be obtained. Although the sample sizes for the control data set is 30 and, test data set is 20, the feature vector $\underline{v}$ for all samples (groups) were found to be normally distributed ensuring optimal results when using discriminant function. The results of this research is very promising, however, further work are needed for verification and validation study with larger sample size.

4.5 Conclusion

The proposed novel texture-based statistical discrimination procedure was shown to be able to detect PNEU, PTB, and LC using chest radiograph. The statistical discrimination procedure studied used wavelet texture measure and the modified principal component (modPC) method. The discrimination procedures consist of (1) pair-wise discrimination for disease present (DP) and disease absent (DA), namely PNEU–NL, PTB–NL, and LC–NL, (2) pair-wise discrimination of diseases, namely PNEU–PTB, PNEU–LC, and PTB–LC, and finally (3) a three population discrimination problems for PNEU, PTB, and LC. Low misclassification probability was achieved when maximum column sum energy texture measure is used for (1), and mean of energy and maximum value texture measures were used for (2) and (3). The maximum column sum energy texture measure yielded 98 % correct classification rates for all three diseases. The diseases were then compared pair-wise and the combination of mean of energy and maximum value texture measures gave correct classification rates of 70, 97, and 79 % for pneumonia, PTB and lung cancer, respectively. The results of this research is very promising, however, further work are needed for verification and validation study with larger sample size.

Acknowledgments We would like to acknowledge the contribution from the Director and staff of The Institute of Respiratory Medicine, Malaysia, and Dr Hamidah Shaban, Selangor Medical Centre. This research was funded under an e-Science Fund grant from the Ministry of Science, Technology and Innovation, Malaysia, Universiti Teknologi Malaysia and University of Malaya.

References

Adam A, Dixon AK (eds) (2008) Grainger & Allison's diagnostic radiology a textbook of medical imaging, vol 1, 5th edn. Elsevier, China

Andrews DF (1972) Plots of high dimensional data. Biometrics 28(125):36

Arzhaeva Y, Tax DMJ, Ginneken B (2009) Dissimilarity-based classification in the absence of local ground truth: application to the diagnostic interpretation of chest radiographs. Pattern Recogn 42:1768–1776. doi:10.1016/j.patcog.2009.01.016

Cherian T, Mulholland EK, Carlin JB, Ostensen H, Amin R, de Campo M, Greenberg D, Lagos R, Lucero M, Madhi SA, O'Brien KL, Obaro S, Steinhoff MC (2005) Standardized

interpretation of pediatric chest radiographs for the diagnosis of pneumonia in epidemiological studies. Bull World Health Organ 83(5):353–359
Daubechies I (1992) Ten lectures on wavelets. SIAM, Pennsylvania
De Veaux RD, Velleman PF, Bock DE (2009) Introduction statistics, 3rd edn. Pearson International, Boston, pp 531–584
Frieden T (2004) Toman's Tuberculosis case detection, treatment and monitoring: question and answer. WHO, Geneva
Ginneken B, Katsuragawa S, ter Haar Romeny BM, Doi K, Viergever MA (2002) Automatic detection of abnormalities in chest radiographs using local texture analysis. IEEE Trans Med Imaging 21(2):139–149
Ginnekien B, ter Haar Romeny BM, Viergever MA (2001) Computer aided diagnosis in chest radiography: a survey. IEEE Trans Med Imaging 20(12):1228–1241
Gonzalez RC, Woods RE (1992) Digital image processing. Addison-Wesley, Reading, p 510
Gopi A, Madhavan SM, Sharma SK, Sahn SA (2007) Diagnosis and treatment of tuberculous pleural effusion in 2006. Chest 131:880–889. doi:10.1378/chest.06-2063
Hamilton W, Peters TJ, Round A, Sharp D (2005) What are the clinical features of lung cancer before the diagnosis is made? A population based case-control study. Thorax 60:1059–1065. doi:10.1136/thx.2005.045880
Hara T, Fujita H, Doi K (2007) Computer aided diagnosis in medical imaging: historical, review, current status and future potential. Comput Med Imaging Graph 31(4–5):198–211
Health Facts (2009) Health Informatics Centre, Planning and Development Division, Ministry of Health Malaysia, May 2009
Homma N, Kawai Y, Shimoyama S, Ishibashi T, Yoshizawa M (2009) A study on the effect of morphological filters on computer-aided medical image diagnosis. Artif Life Robot 14:191–194. doi:10.1007/s10015-009-0651-8
Johnson RA, Wichern DW (2007) Applied multivariate statistical analysis, 6th edn. Pearson International Edition, New Jersey
Katsuragawa S (2007) Doi K Computer-aided diagnosis in chest radiography. Comput Med Imaging Graph 31:212–223. doi:10.1016/j.compmedimag.2007.02.003
Malaysian Cancer Statistics (2006) Data and figure peninsular Malaysia 2006, Ministry of Health Malaysia
Mardia KV, Kent JT, Bibby JM (1979) Multivariate analysis. Academic Press, London
Middlemiss H (1982) Radiology of the future in developing countries. Br J Radiol 55:698–699
Moores BM (1987) Digital X-ray imaging. IEE Proc 134(2):115 (Special issues on medical imaging)
Nakamura K et al (1970) Studies on the diagnostic value of 70 mm radiophotograms by mirror camera and the reading ability of physicians. Kekkaku 45:121–128
TB a Problem Once Again. New Straits Time article, 29 March 2008
Noor NM, Rijal OM, Yunus A, Abu-Bakar SAR (2010) A discrimnation method for the detection of pneumonia using chest radiograph. Comput Med Imaging Graph 34:160–166. doi:10.1016/j.compmedimag.2009.08.005
Oliveira LLG, e Silva SA, Ribeiro LHV, de Oliveira RM, Coelho CJ, Andrade ALSS (2007) Computer-aided diagnosis in chest radiography for detection of childhood pneumonia. Int. J Med Inform. doi:10.1016/j.ijmedinf.2007.10.010
Schillham AMR, van Ginneken B, Loog M (2006) A computer aided diagnosis system for the detection of lung nodules in chest radiographs with an evaluation on a public database. Med Image Anal 10(2):246–258
Sonka M, Hlavac V, Boyle R (1998) Image processing, analysis, and machine vision. International Thomson Publishing, Pacific Grove, p 652
van Ginneken B, Katsugarawa S, ter Haar Romeny BM, Doi K, Viergever MA (2002) Automatic detection of abnormalities in chest radiographs using local texture analysis. IEEE Trans Med Imaging 21(2):139–149
Walker JS (1999) A primer on wavelets and their scientific applications. Chapman and Hall/CRC Press, Boca Raton

WHO (2003) International agency for research on cancer. In: Steward BW, Kleihues P (eds). World Cancer Report. WHO, Geneva

WHO (2006) The global plan to stop TB 2006-2015: action for life towards a world free of tuberculosis. WHO, Geneva

WHO Report (2004) Global tuberculosis control, surveillance, planning, financing. WHO, Geneva

Wipf JE, Lipsky BA, Hirschmann JV, Boyko EJ, Takasugi J, Peugeot RL, Davis CL (1999) Diagnosing pneumonia by physical examination: relevant or relic? Arch Intern Med 139:1082–1087